

Automated vessel segmentation from quantitative susceptibility maps at 7 Tesla

Pierre-Louis Bazin¹, Audrey Fan², Gabriela Mianowska³, Agnieszka Olbrich³, Andreas Schäfer¹, Arno Villringer¹, and Claudine Gauthier⁴

¹Max Planck Institute for Human Cognitive and Brain Sciences, Leipzig, Germany, ²Stanford University, California, United States, ³AGH University of Science and Technology, Cracow, Poland, ⁴Concordia University, Montréal, Québec, Canada

Target audience: Neuroscientists and clinicians interested in neurovasculature and brain metabolic physiology.

Purpose: Baseline oxygen extraction fraction (OEF) is an important physiological parameter to understand brain function, and it is known to be affected in diseases such as stroke and cancer.^{1,2} MRI measures of local OEF values therefore hold great promise for the study of healthy and pathological brain physiology. Regional OEF values can be obtained from susceptibility measurements in small cortical veins³, although this method is currently limited by the fact that manual segmentations of vessels are necessary to identify smaller cortical veins on MR venograms. Here we present a method for segmenting vasculature from quantitative susceptibility maps through use of oriented shape filters and a Markov Random Field (MRF) diffusion algorithm.

Methods: Eight human subjects were scanned on a 7-T Siemens MR system with a 24-channel head coil. Susceptibility-weighted images (SWI) were acquired with flow compensation along all three axes⁴ at 0.6 mm isotropic resolution with TR=23ms; TE=7.5ms; matrix = 320x320x104; GRAPPA acceleration R=3; and scan time=4min. Quantitative susceptibility mapping (QSM) was performed using a fast regularization reconstruction described in.⁵ A dedicated segmentation algorithm was developed to perform automated vessel segmentation in two steps. First, thin tubular structures are estimated locally with a directional shape filter at the voxel resolution. Second, a sparse MRF is built from the filter responses and their neighbors in the strongest response direction. The local filter responses are then combined over the length of the vessels with a fast diffusion technique to strengthen responses along true vessels. OEF values were then extracted from the susceptibility difference between segmented vessels and CSF ($\Delta\chi_{\text{vein-CSF}}$) using the relationship $\text{OEF} = \Delta\chi_{\text{vein-CSF}}/(4\pi \cdot 0.27\text{ppm} \cdot Hct)$, where $Hct = 0.4$ is the assumed blood hematocrit.³ Manual delineations of vessels were obtained for one subject by two raters from the QSM. For comparison, one rater also delineated the vessels from the SWI. Automated and manual segmentation methods were compared separately and using a STAPLE⁶ consensus of the manual delineations.

Results: Segmentations obtained are presented in Fig. 1. Regions at the boundary of the cortex were masked in the QSM reconstruction. Comparisons to manual delineations (Fig. 2) show that the automated method performs similarly to human raters in terms of Dice overlap and slightly better in terms of average distance. Segmentation on QSM or SWI data provides comparable results, although QSM results appear better resolved. OEF measurements (Fig. 3) based on the vessel segmentations are within physiological range and appear stable between subjects.

Discussion: High resolution vasculature data is challenging to obtain with full-brain imaging techniques. QSM provides an alternative contrast to depict venous vessels in high-resolution images, which is not impacted by signal variations due to relaxation parameters or non-local field perturbations seen in phase images and SWI. The proposed segmentation method provides a fast segmentation result comparable to manual segmentations, a particularly long and tedious task for smaller cortical vessels.

References

1. Heiss et al., Early [(11)C]Flumazenil/H(2)O positron emission tomography predicts irreversible ischemic cortical damage in stroke patients receiving acute thrombolytic therapy, *Stroke* 31 (2000): 366–369.
2. Nordsmark et al., Prognostic value of tumor oxygenation in 397 head and neck tumors after primary radiation therapy. An international multi- center study, *Radiat Oncol* 77 (2005): 18–24.
3. Fan et al., Quantitative oxygenation venography from MRI phase, *Magn Reson Med* 2014;72(1):149-159.
4. Deistung et al., ToF-SWI: Simultaneous time of flight and fully flow compensated susceptibility weighted imaging, *J Magn Reson Imaging* 2009;29(6):1478-1484.
5. Bilgic et al., Fast quantitative susceptibility mapping with L1-regularization and automatic parameter selection, *Magn Reson Med* 2014;72(5):1444-1459.
6. Warfield et al., Simultaneous truth and performance level estimation (STAPLE): an algorithm for the validation of image segmentation, *IEEE Trans Med Imaging*. Jul 2004; 23(7):903-921.

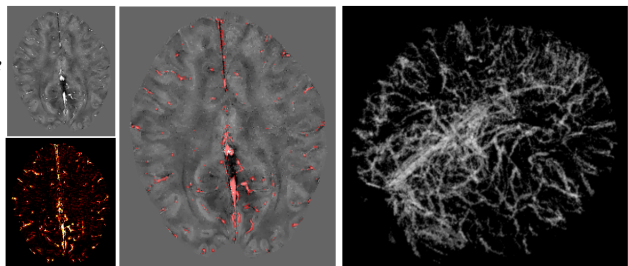


Fig. 1: Segmentation example: top left, reconstructed QSM; bottom left, estimated vessel probabilities; center, segmented vessels over the QSM data; right 3D rendering of the segmented vessels.

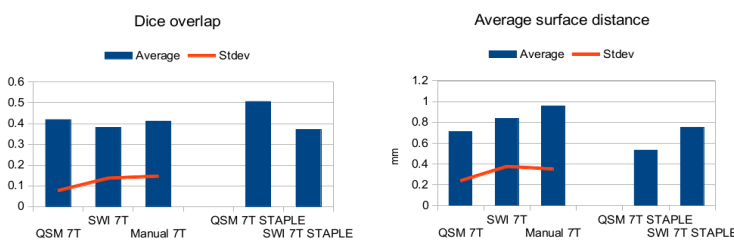


Fig. 2: Comparison of automated and manual segmentations: left, comparing the automated method based on QSM, SWI and the manual delineations against each (other) manual delineation; right, comparing the automated method to the STAPLE consensus manual delineation.

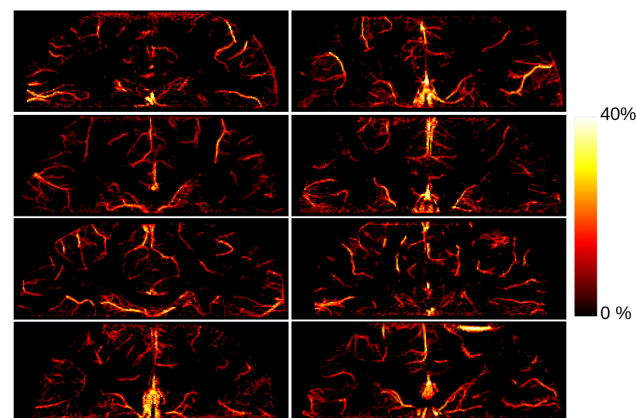


Fig. 3: Oxygen extraction fraction (OEF) measured for all eight